Scattering of Cherenkov Radiation Produced by UHE Neutrino Interactions in the Antarctic Ice Cap

Erik Everson

September 18, 2005

Abstract

The goal of the ANITA project is to detect neutrino interactions within the Antarctic ice cap. To do so, a radio antenna is used to detect radiation produced by the interaction. The radiation is scattered as it passes through the rough Antarctic surface. Power distributions of light through wavelength scale rough ground glass diffusers are investigated in hopes of understanding how the power distribution shifts, broadens, and drops with roughness and incident angle.

1. Introduction

The Antarctic Neutrino Impulse Transient Antenna (ANITA) project is designed to detect radio emissions produced by neutrino interactions within the Antarctic ice cap. An incoming ultra high energy neutrino weakly interacts with the neutrons and protons in the ice, producing a net charged particle shower. The resulting particle shower moves faster than the speed of light within the ice and, hence, emits a radio pulse, Cherenkov radiation. The emitted Cherenkov radiation propagates out in a 57^{o} cylindrically symmetric cone about the neutrino's original path, see figure 1. The cone has a divergence of about 1.5^{o} and has a bandwidth of 0.3 meters to 1.0 meter.

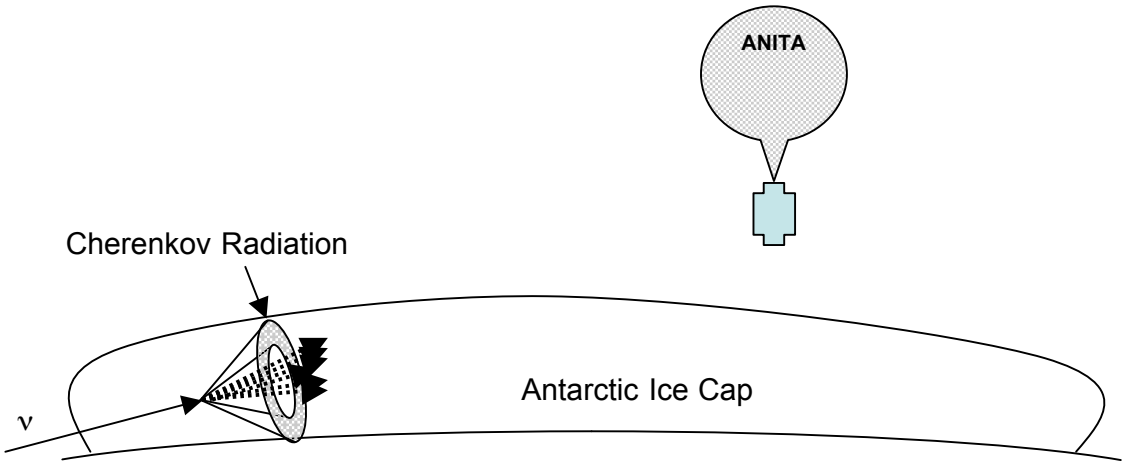

Figure 1: A neutrino enters the ice cap and produces a particle shower. The resulting shower emits a cone of radiation, Cherenkov radiation.

The success of the project depends on our ability to detect the emitted Cherenkov radiation. A radio antenna is flown about 40 km above the Antarctic surface along the

80^{o} S latitude, so the emitted radiation must first pass through the Antarctic surface before it reaches the detector. There is some dispersion of the radiation as it travels through the bulk because of a changing index of refraction. In the deep parts of the ice cap the index of refraction is about 1.8, but near the top it linearly changes from 1.8 to 1.3. However, our concern is how much dispersion is caused when the radiation passes through the snow-air boundary at the surface. If the surface was perfectly smooth there would not be a problem, but there are features on the surface that range in scale on the order of the wavelength of the radiation. So the question we want to ask ourselves is: what kind of scattering effects arise when radiation passes through a diffusing surface that has roughness scales on the order of the wavelength of the radiation?

2. Experiment and Simulation

We can not directly test the situation in Antarctica, so we devised a scaled down experiment that we could test in the lab. Along side the experiment, we developed a computer simulation that could be compared to the experimental data. In the end we hope to gain a good agreement between the simulation and experimental data, so then we could set the parameters for Antarctica and test the situation.

3.A Experiment

For this experiment, the situation in Antarctica has been scaled down to the wavelength of a He-Ne laser, 632.8 nm. To simulate the surface of Antarctica we chose to use 400 grit, 1000 grit, and 1500 grit ground glass diffusers. Unfortunately, at this time we do not have the means of measuring the height variations or lateral length scales of the diffuser. However, according to ref. [1] a 1500 grit diffuser has an RMS height variation of about 622 nm, or ~λ. The 1000 grit has an RMS height variation of ~2λ and the 400 grit has an RMS height variation of ~4λ. Future measurements will be taken to test these values and examine the lateral length scales.

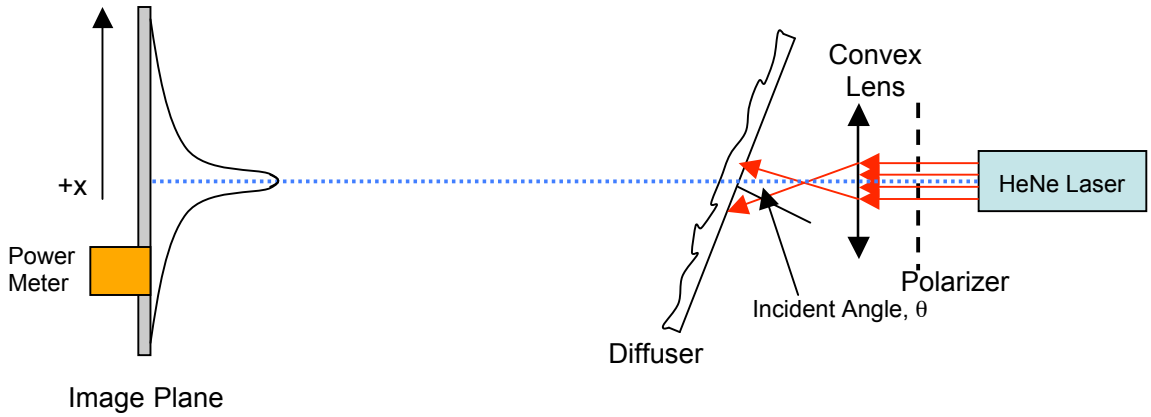

Figure 2: Experimental apparatus.

Figure 2 contains the experimental setup. Since the Cherenkov radiation is incident on the Antarctic surface with a random polarization, we first send the laser through a polarizer to test what effects vertically polarized light versus horizontally polarized light

has on the image. To simulate the divergence of the radiation, the polarized light is sent through a 25 mm focal length convex lens to produce a 1.55^o diverging beam.

In the apparatus we chose to rotate the diffuser through a range of 0^o to 70^o so the center of the image is always centered at the specular point, or specular angle. The specular angle is the angle the light will be most concentrated if the beam was incident on a flat piece of glass. If the beam is incident at an angle θ, then by Snell's Law the beam will exit the flat glass at the same angle; thus, the specular angle is the same as the incident angle.

There are significant differences between this experiment and the situation in Antarctica. First, monochromatic light is used in the experiment, whereas the radiation in Antarctica has a band width. The monochromatic light causes the power distribution to have a speckle pattern [2], but a bandwidth makes the power distribution more continuous. Second, In Antarctica the source of the radiation comes from within the medium, but for this experiment the source comes from outside the medium. This means that, in the experiment, we are unable to have incident angles on the diffusing surface greater than the critical angle, but in Antarctica it is possible to have incident angles greater than the critical angle. See chart 1 for conversion of incident angle to actual incident angle on the diffusing surface for a diffuser of index of refraction of 1.5.

Incident Angle	**Incident Angle of Diffusing Surface**
0^o	0.0^o
10^o	6.6^o
20^o	13.2^o
30^o	19.5^o
40^o	25.4^o
50^o	30.7^o
60^o	35.3^o
70^o	38.8^o

Chart 1: Conversion chart of incident angle to incident angle on diffusing surface for a source originating outside a diffuser of index of refraction of 1.5.

3.B Simulation

The most important part of the simulation is constructing a diffuser contour that properly models the surface characteristics of a real diffuser. To do this I started with a square area of fixed length and divided it into bins. Each bin is originally given a fixed height of one, which will become the mean height of the diffuser. Then the height of each bin is randomly varied according to a Gaussian distribution,

$$h = 1 + \sin(2\pi x)\left[\sigma\sqrt{-2\ln(z)}\right] \qquad (1)$$

where σ is the standard deviation of the distribution, x is a randomly generated number between zero and one, and z is a randomly generated number between $\exp(1/2\sigma^2)$ and

one. By choosing this range for *z* the height varies from zero to two with one being the mean height. To give the height of the contour dimensions just multiply by amplitude $A/2$, so the maximum height is A and the mean height is half of A. Now, by changing the standard deviation of the distribution the RMS height of the contour can be selected, essentially selecting the roughness of the diffuser. A small σ will produce very small variations and a small RMS height, while a large σ will produce large variations and a large RMS height.

There are actually two features that contribute to the roughness of the contour. The first is the RMS height of the contour, which has already been discussed. The second contributor is the lateral length scales, which can be controlled by varying the bin widths of the contour.

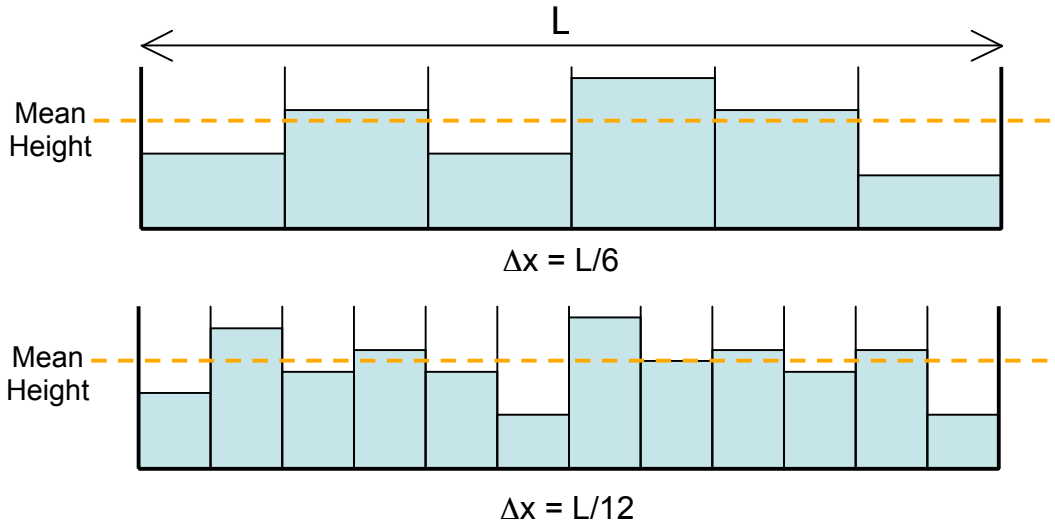

Figure 3: One dimensional boundary. Because the slopes increase like $1/\Delta x$, the roughness increase with decreasing bin width

Consider a one dimensional boundary of length L, see figure 3. First, divide the boundary into six bins then the bin width is L/6. Now, generate height variations with a fixed σ so the boundary has a fixed RMS height. Repeat this process with the same σ, but divide the length into twelve bins so the bin width is L/12. Since the height variations were generated with the same σ, they both have the same RMS height. However, the second boundary is rougher because it has steeper slopes. The rise in the slope is the same for each contour, but the run for the second case is a factor of two smaller so it tends to have steeper slopes. The steepness of the slopes is important because it causes more refraction and, hence, more scattering of the light.

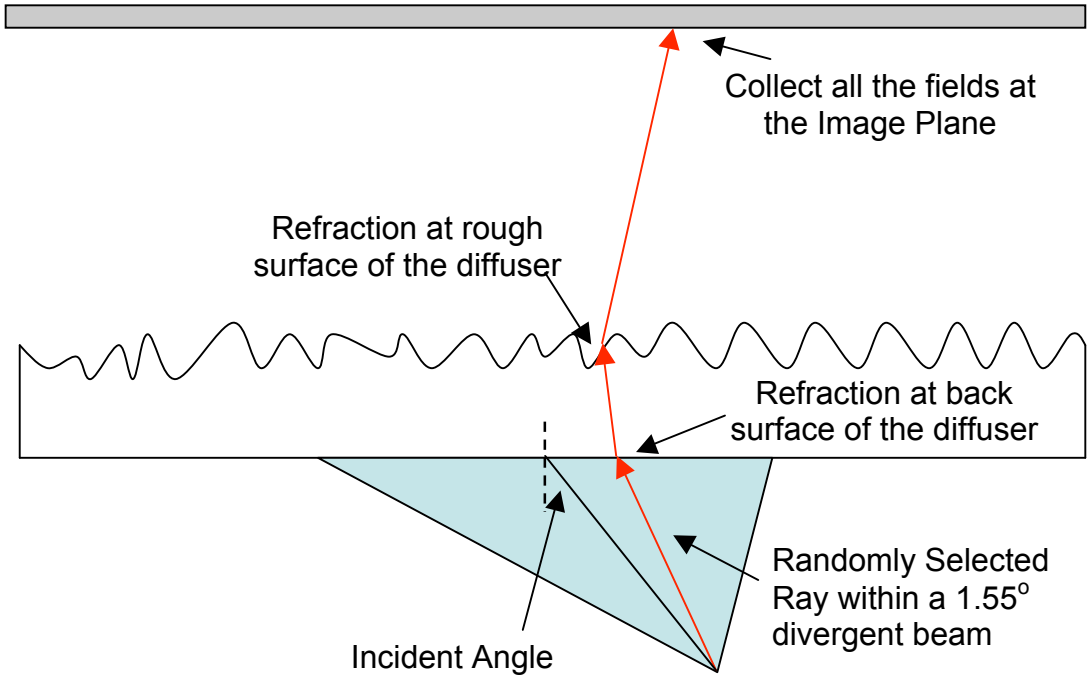

Figure 4: Ray tracing.

The simulation is setup to only test the effects of refraction according to Snell's Law and phase differences. It does not include Fresnel coefficients for polarizations or first order reflections off the diffusing surface; these will be implemented in the next model. Ray tracing is the simplest model to start with and, for additional simplicity, the fields are assumed to be scalar, but this would have to be changed when Fresnel coefficients are included. The simulation starts by randomly generating a ray within a 1.55^{o} diverging cone, see figure 4. Keeping track of the phase, the ray is followed through refraction on the back surface of the diffuser, up to the front surface, refraction through the diffuser surface, and up to the image plane. This is done for an N number of rays. Then the field from each ray is summed up into the bin of the image that it strikes and square to get the power.

3. Experiment Results

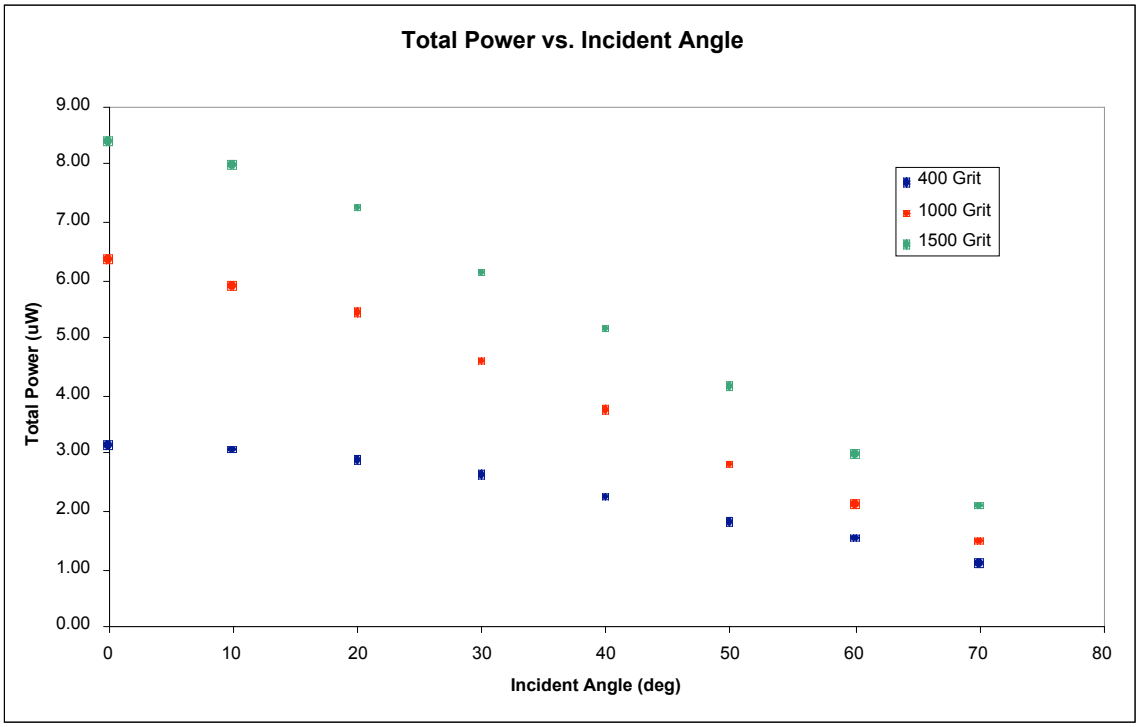

Figure 5: Total power versus roughness and incident angle.

For this experiment we are interested in determining how the power distribution of the image of vertically polarized light changes versus roughness and incident angle. For flat glass all the power is always concentrated in the specular point of the power distribution for all incident angles. So the power distribution looks like a spike at the specular angle. At normal incidence the power of the specular point, total power, is 102.91 μW and falls to 65.51 μW at 70^{o} incidence. Replacing the flat glass with any one of the diffusers causes the total power to significantly decrease, see figure 5. For the 1500 grit diffuser the power drops to 8.38 μW at normal incidence, while the 400 grit drops to 3.14 μW and the 1000 grit drops to 6.36 μW. As the incident angle is increased the total power continues to drop. For the 1500 grit and 1000 grit diffusers the total power drops by a factor of about 4 at 70^{o} incidence, while the 400 grit drops by a factor of about 3. It is likely that most of the power is loss comes from total internal reflection within the diffuser and reflection of the back surface.

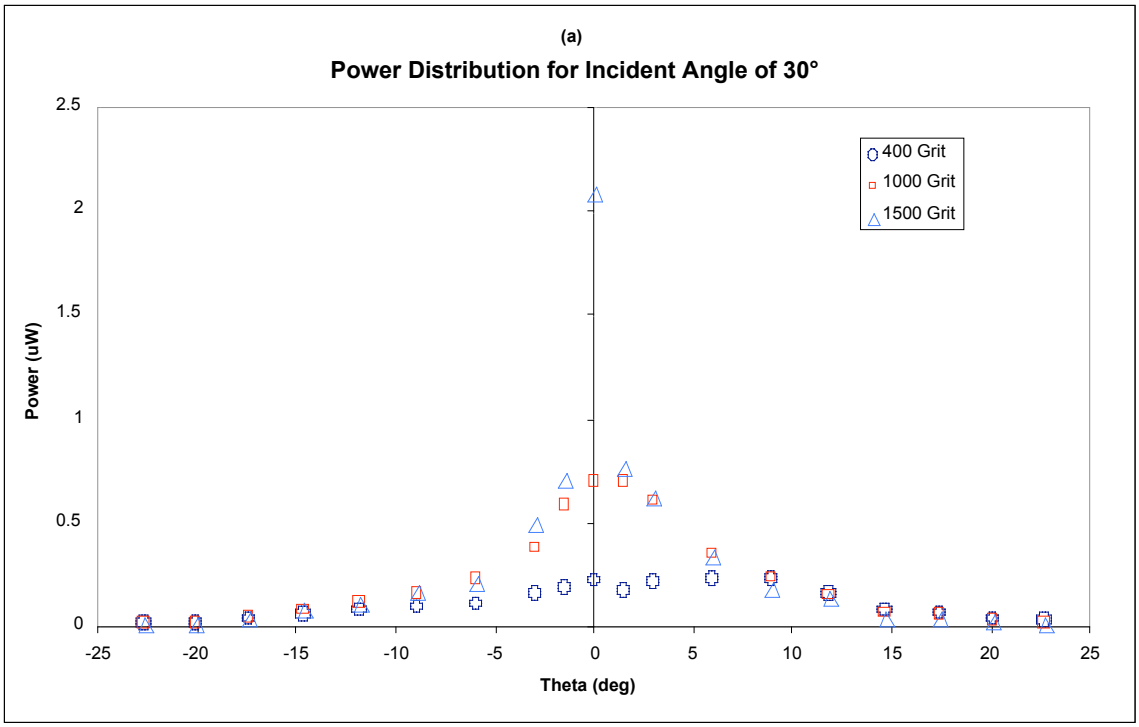

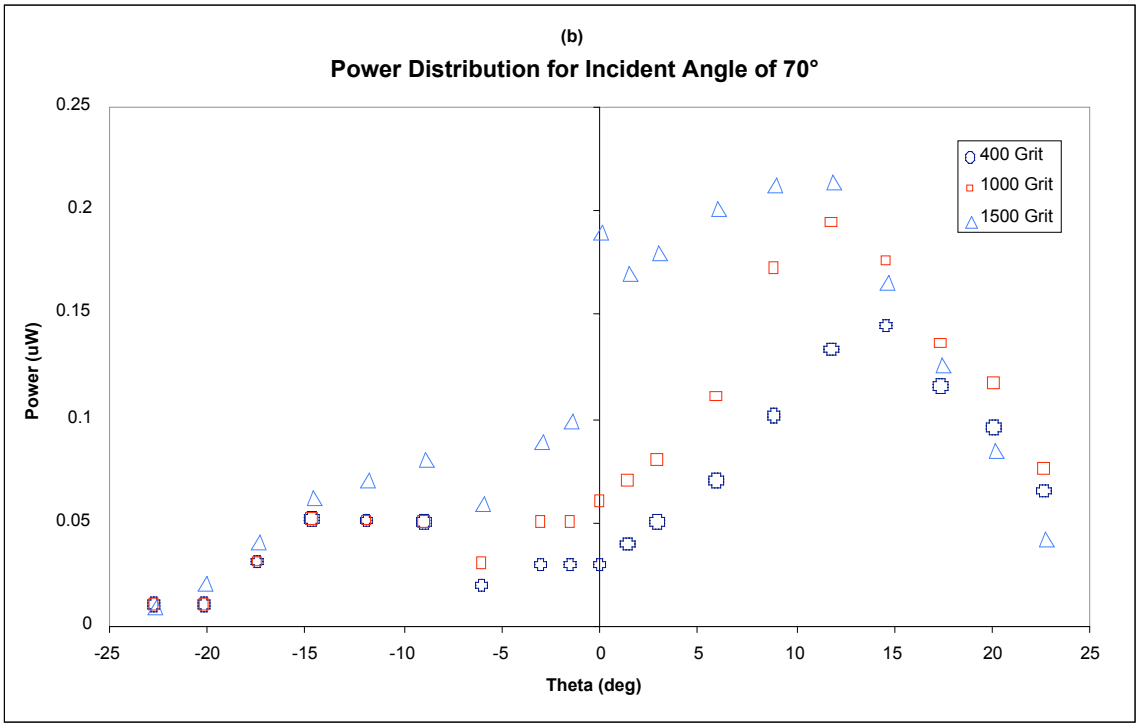

Figure 6: (a) overlay of power distribution for an incident angle of 30° (b) overlay of power distribution for an incident angle of 70°

In addition to the decrease in power, we found that at high incident angles and rougher diffusers that the power distribution became asymmetrical about the specular angle. Looking at an incident angle of 30°, see figure 6a, it can be seen that at larger roughness the specular peak significantly drops and the power seems to be scattered more

towards positive angles, towards the diffuser normal. This forward scattering is even more prominent at larger incident angles, see Figure 6b. The power distribution also tends to broaden with increasing roughness and incident angles.

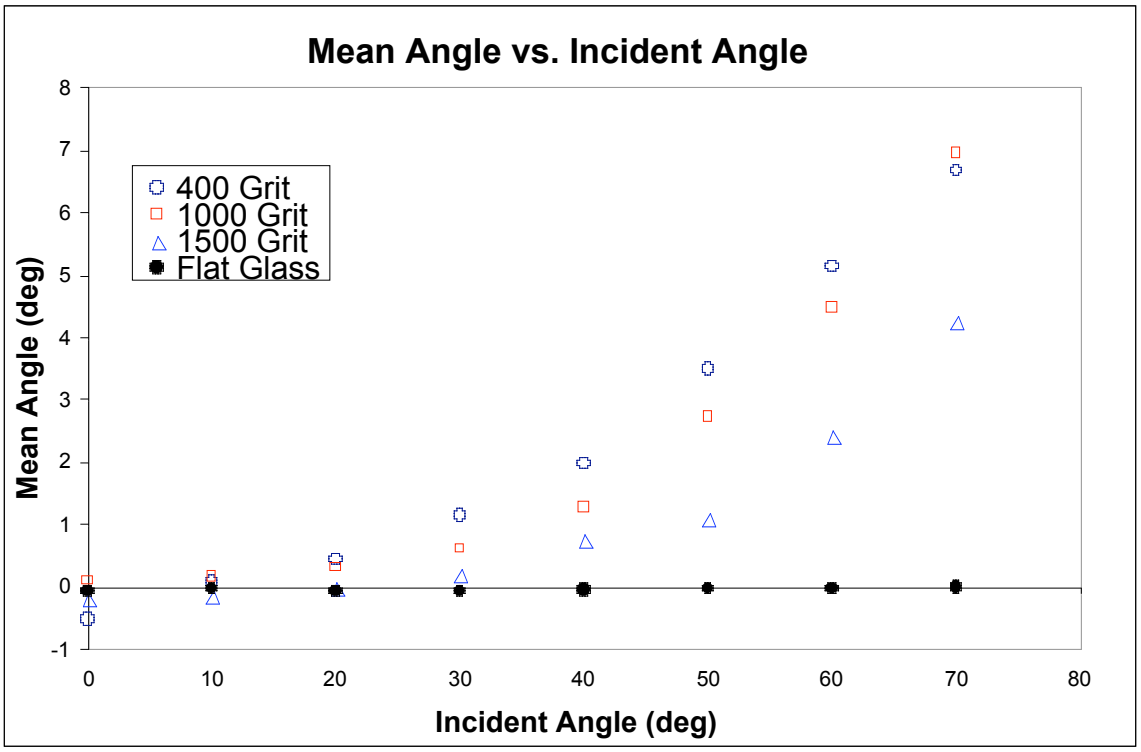

Figure 7: Mean transmission angle vs. Incident Angle and Roughness

To quantize the shift of the power distribution we can look at the mean angle of the distribution. The mean angle is just a weighted average of the transmission angle

$$\bar{\theta} = \frac{\sum \theta \cdot P(\theta)}{\sum P(\theta)} \qquad (2)$$

where θ is the transmission angle and P(θ) is the power at θ. A mean angle of zero would indicate that the power distribution is centered about specular angle. Figure 7 shows that at large incident angles and roughness that the mean angle is shifted towards positive angles. However, for flat glass the mean angle stays close to zero, as expected.

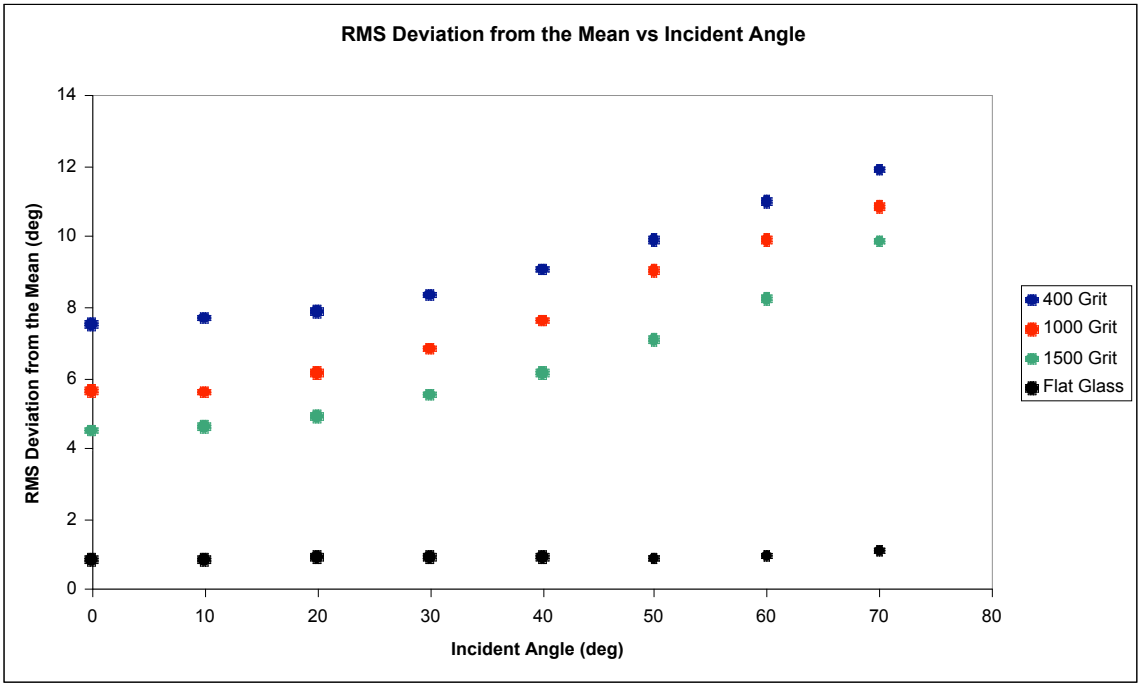

Figure 8: RMS angle vs. Incident Angle and Roughness

We can quantify the spread of the distribution by examining the RMS transmission angle from the mean. Figure 8 shows that the spread of the distribution increases with increasing incident angle and roughness. By Snell's Law, a group of rays incident at large angles will be spread out more than a group of rays at smaller incident angles. So for larger incident angles it makes sense that the power distribution tends to be more spread out. Now, for rougher diffusers the slopes of diffuser boundary are much steeper, so the incident angles of the light on this boundary increase for increase in roughness.

4. Simulation Results

The simulation was set up to run with a 1500 grit diffuser, so the RMS height of the diffusing surface was set to 622 nm. Recall that the bin size of the diffuser also contributes to the roughness of the diffuser. A bin size of 6 microns was chosen because it produced results near those of the experimental results. These parameters should be adjusted once actual measurements of the diffuser surface can be made.

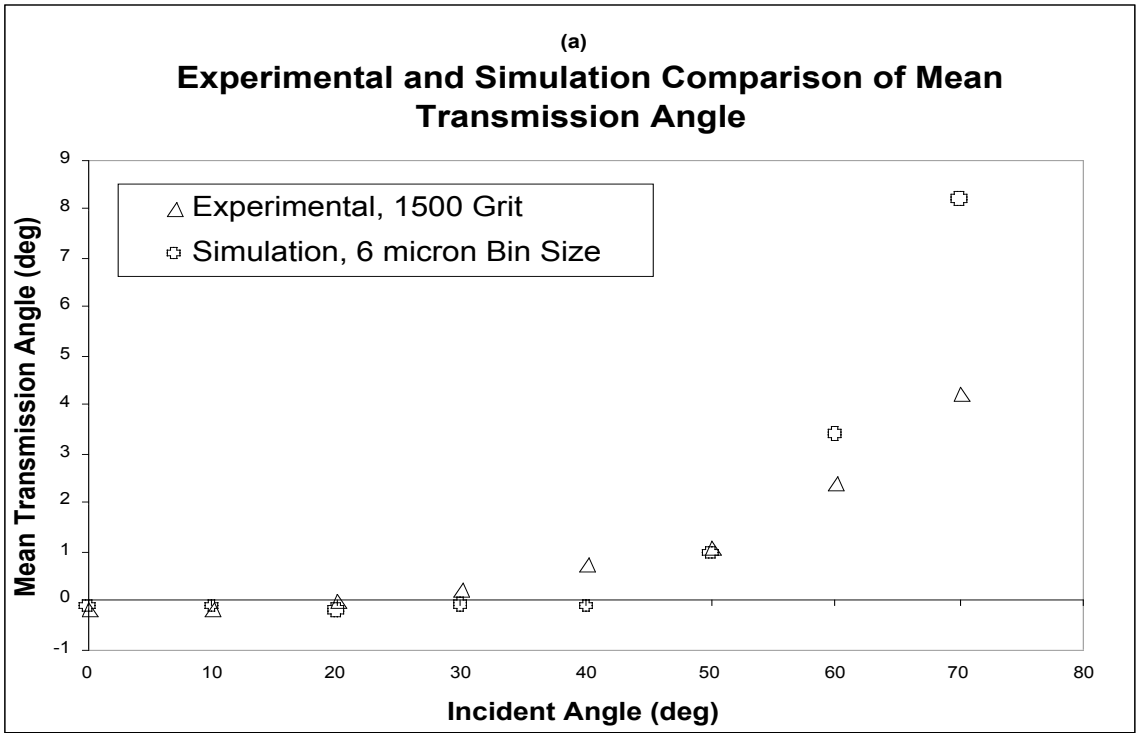

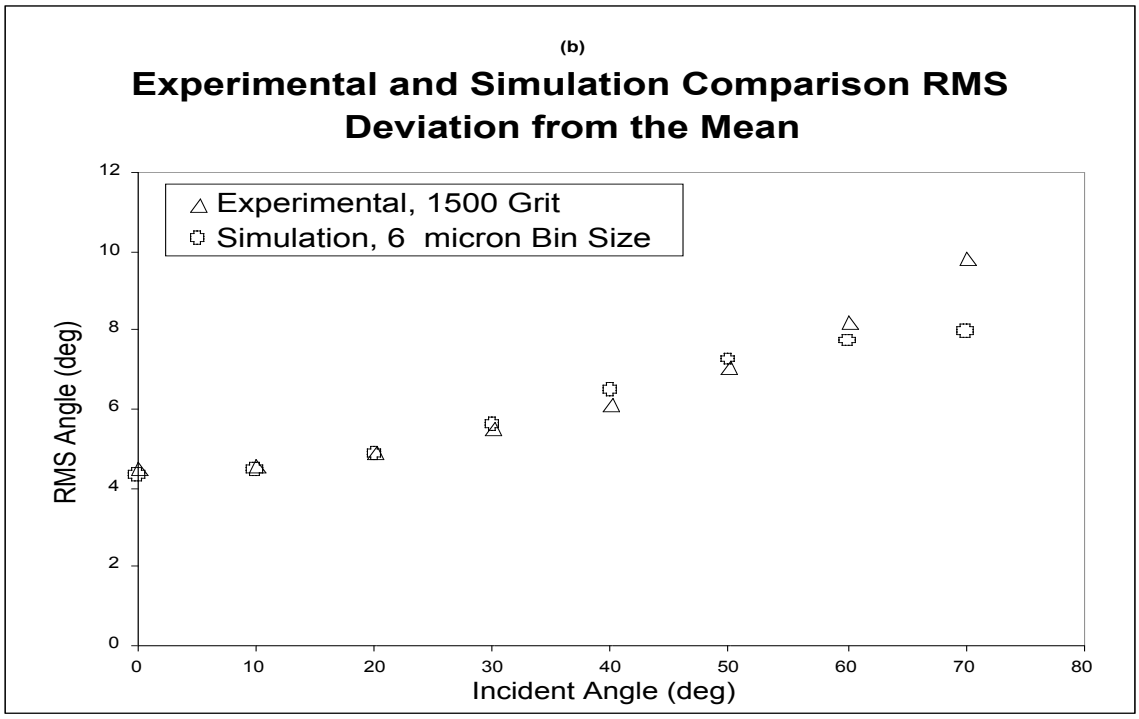

Figure 9: (a) Mean Transmission Angle simulation results compared to experimental results for a 1500 grit diffuser. (b) RMS Angle simulation results compared to experimental results for a 1500 grit diffuser.

The mean angle of the simulation results at low incident angles is near zero, which agrees with experimental results. This makes sense because at low angles the beam passes through boundaries of both negative and positive slopes so the rays are refracted

symmetrically about the specular angle. At higher incident angles the simulation produces a larger mean angle, more forward scattering, see figure 9a. At higher angles the rays do not pass equally through positive and negative slopes. For example, if the beam is incident towards the positive x-axis it will only refract through negative slope boundaries, but if it is incident towards the negative x-axis then it will only pass through positive slope boundaries. By Snell's Law, these rays are refracted away from the normal to the boundary but towards the normal of the diffuser and could account for the forward scattering of the light. However, at a 70^{o} incident angle the simulation produced much more forward scattering than the experiment. This could be contributed to first order reflections in the diffuser. In the experiment there is a considerable amount of total internal reflect at high incident angles. If total internal reflect is implement in the simulation then when the reflected ray is incident on the diffusing surface for the second time will be projected towards the negative transmission angles. This effect could bring the mean transmission angle down at higher incident angles, but would not significantly affect low incident angles because of the equal incidences on negative and positive slopes.

The simulation results for the RMS angle closely matches the experimental results except at high incident angles, see figure 6b. The decrease in RMS angle at high incident angles could be contributed to total internal reflection. At high incidence there are a significant number of reflected rays and, since the simulation ignores these rays, they do not go into making up the image. If the reflected rays were to pass through the boundary on their second attempt then the power distribution would broaden out, producing a larger RMS angle.

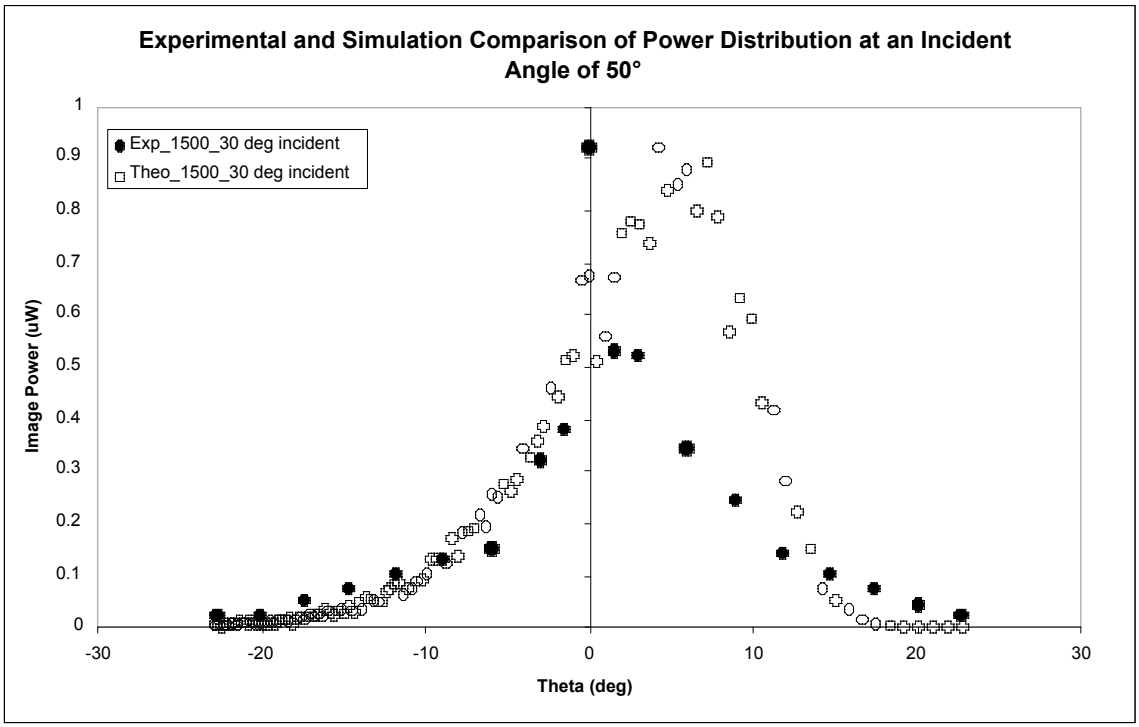

Figure 10: Overlay comparison of the experimental and simulation power distributions for a 1500 grit diffuser incident at 50^{o}.

In addition to producing accurate mean transmission and RMS angles, the simulation needs to be able to produce comparable power distributions to the experimental results. Unfortunately, this is not the case at the moment. At an incident angle of 50^{o} the simulation power distribution has a much lower specular peak and a more prominent forward scattering peak, whereas the experimental distribution still has a very prominent specular point, see figure 10.

5. Conclusion

Steps have been made to further understand of the problem in Antarctica but further investigation still needs to be done to get conclusive results. All hope is not lost though. If similar power distributions are produced in Antarctica, then it may actually increase our ability to detect the Cherenkov radiation. The forward scattering would bring the radiation into the region of the detector and the broadening of the power increases the detectable region. However, if the power drops too much then that would hinder our ability to detect the radiation. This also makes it harder to trace back where the interaction occurred.

We still have to consider that there is a significant difference between the experiment in the lab and the situation in Antarctica. In the lab we have the source of our radiation coming from outside the medium, but in Antarctica the source comes from within the medium. This could lead to slight discrepancies; that is why we need and accurate simulation. If we get a working model for the case in the lab then it can be modified for the situation in Antarctica.

Currently, the simulation is showing progress but several modifications need to be made before we can use it for ANITA. First, first order reflections should be implemented because they may have a significant effect on the power distribution at high incident angles. Second, Fresnel coefficients should be considered to test the effects of different polarized beams. By implementing Fresnel coefficients a reflected ray is generated for every transmitted ray so this could also have a significant effect on the image. If the ray tracing model does not work, then the next step is to try Huygens' Principle. By using a Huygens' model not only are refraction and phase effects explored but diffraction is also considered.

6. Acknowledgements

I would like to thank Professor David Saltzberg and Amy Connolly for all their support and guidance through this research opportunity. I would also like to thank Brian Daub for his assistance in the lab, NSF for funding the REU, and Françoise Queval for organizing and developing this program.

References

[1] Duje Tadin, Richard F. Haglund, Jr., Joseph S. Lappin, R. Alan Perers, *Effects of surface microstructure on macroscopic image shading*, [unpublished]

[2] L. G. Shirley and N. George, "Diffuser Radiation Patterns Over a Large Dynamic Range. 1: Strong Diffusers," Appl. Opt. **27**, 1850 (1988)

[3] Amy Connolly, personal communication

[4] David Saltzberg, personal communication